The alveolar type II cell-specific functions of EP300 in pulmonary fibrosis

Soo Yeon Lee

Department of Medical Science

The Graduate School, Yonsei University

The alveolar type II cell-specific functions of EP300 in pulmonary fibrosis

Soo Yeon Lee

Department of Medical Science

The Graduate School, Yonsei University

The alveolar type II cell-specific functions of EP300 in pulmonary fibrosis

Directed by Professor Ho-Geun Yoon

The Doctoral Dissertation

submitted to the Department of Medical Science

the Graduate School of Yonsei University

in partial fulfillment of the requirements for the degree of Doctor of Philosophy

Soo Yeon Lee

December 2020

This certifies that the Doctoral Dissertation

of Soo Yeon Lee is approved.

Thesis Supervisor: Ho-Geun Yoon

Thesis Committee Member#1: Myung Hyun Sohn

Thesis Committee Member#2: Jae Myun Lee

Thesis Committee Member#3: Moo Suk Park

Thesis Committee Member#4: Hyo Sup Shim

The Graduate School

Yonsei University

December 2020

ACKNOWLEDGEMENTS

박사 학위를 받기까지 응원해주시고 지도해주신 많은 분들께 감사의 말씀을 드립니다. 먼저 지도교수님으로써 이끌고 가르쳐 주신 윤호근 교수님께 큰 감사의 마음을 전합니다. 부족한 저를 제자로 받아주시고 잘 인도해주셔서 졸업까지 무사히 마칠 수 있었습니다. 인내심을 가지고 지켜봐주시고 많은 기회를 주시고 때론 질책해 주심으로써 바른 길로 올 수 있었습니다. 교수님께 배운 지식과 자세를 바탕으로 좋은 연구자가 되도록 노력하겠습니다. 그리고 저의 빈약한 가설도 긍정적으로 검토해주시고 예리하게 지적해주신 손명현 교수님, 이재면 교수님, 박무석 교수님, 심효섭 교수님께 감사드립니다. 교수님들께서 관심을 가지고 좋은 방향으로 이끌어주셔서 제 학위논문을 완성할 수 있었습니다. 그리고 생화학 교실의 김경섭 교수님, 허만욱 교수님, 김건홍 교수님, 박상욱 교수님, 김재우 교수님, 전경희 교수님께 감사의 말씀을 전합니다.

우리 실험실의 구성원 여러분께도 고마운 마음을 전합니다. 제 학위과정의 시작과 끝을 모두 지켜보고 응원해준 유일한 사람인 수연언니, 정말 진심으로 감사합니다. 언니가 없었으면 제 학위과정은 더 힘겨웠을 것이라 생각이 듭니다. 그래서 학문적으로나 정신적으로 많은 힘이 되어준 언니께 다 표현하기도 힘들만큼 큰 고마움을 느낍니다. 감사합니다. 또 바쁘신 와중에도 많은 조언과 지원을 해주신 미정언니와 정윤오빠께도 감사드립니다. 현식이와 경은이, 재환이는 어린 나이에 실험실에 들어와 적응하기가 힘들었을 텐데 잘 적응해주어 고맙고 내가 선배들에게 받은 지도와 애정을 온전히 전해주지 못한 것 같아 아쉬움이 남습니다. 지금은 실험실을 떠나 각자의 자리에서 최선을 다하고 있는 실험실원들에게도 고마움을 전합니다. 재성오빠, 미현언니, 승현오빠,

가람오빠는 제가 막내로 있던 2년동안 선배로서 많은 지식과 조언, 격려 해주셔서 감사했습니다. 정말 값진 시간이었고 언니 오빠들을 알고 지낸것만으로도 운이 좋았다는 생각이 듭니다. 어디에 계시든 건강하고 하는 일 다 잘 되길 바라겠습니다. 모두의 도움이 없었다면 이 학위 논문이 완성될 수 없었다는 점에 재차 함께하고 있는 구성원 여러분께 감사의 말을 전합니다.

생화학 교실 구성원들에게 또한 감사의 마음을 전합니다. 학부 선배로써 격려와 응원해주신 혁구오빠, 잘 될 거라며 응원해준 서현언니와 입학 동기인 다현이에게 감사드립니다.

학위 과정동안 많은 응원과 격려를 보내준 친구들에게도 고마운 마음을 전합니다. 자주 보진 못하지만 만날 때마다 응원해주고 격려해준 상지, 수민, 유나 고맙습니다. 또 같은 분야에 있어서 의지도 되고 서로에게 자극도 되어준 누리, 희환, 새얀, 현경, 인영이 고맙습니다. 그리고 긴 시간동안 변함없이 지지해주고 묵묵히 옆에서 응원해준 준일이에게 감사합니다.

긴 시간 동안 저를 믿고 저의 든든한 지원군이 되어준 부모님께 감사한 마음을 전합니다. 수년간 저에게 주신 사랑과 지지 그리고 인내 덕분에 제가 무사히 학위과정을 마칠 수 있었습니다. 저를 위해 해주시는 조언과 말씀은 제가 어느 방향으로 가고 선택할지 알려주는 등대와 같습니다. 정말 감사합니다. 그리고 마음 속 깊이 부모님을 존경하고 사랑합니다. 앞으로도 건강하게 오래 함께 있어주세요.

다시 한번 학위 논문이 나오기까지 응원해주신 모든 분들께 감사의 마음을 전합니다.

TABLE OF CONTENTS

LIST OF FIGURES

Abstract

The alveolar type II cell-specific functions of EP300 in pulmonary fibrosis

Soo Yeon Lee

Department of Medical Science

The Graduate School, Yonsei University

(Directed by Professor **Ho-Geun Yoon**)

Idiopathic pulmonary fibrosis (IPF) is characterized by chronic progressive parenchymal lung fibrosis. The lungs of IPF patients display a characteristic fibrosis, characterized by deposition of extracellular matrix (ECM), which results in

distortion of normal lung structures and loss of respiratory function. Although extensive researches for IPF pathogenesis have been reported for several decades, the precise mechanisms are still unknown and the specific treatments for elimination of fibrosis and prolongation of survival are also still unsolved. In this study, the increased expression of EP300 was observed in lung of patients with IPF and in the mouse models of lung fibrosis. Lung fibrosis was significantly diminished by alveolar type II (ATII) cell-specific deletion of EP300 genes. However, genetic deletion of EP300 in the lung epithelial club cells (*Ccsp-Ep300*$^{d/d}$) had no effects on the lung fibrosis, suggesting that ATII-specific EP300 plays important role in lung fibrosis progression. RNA-sequencing and ChIP-sequencing analyses identified CCL2 and CCL7 as a direct target of EP300 in both ATII cells and mice. By analyzing Chromatin immunoprecipitation assay in mouse tissue, it was demonstrated that binding of EP300 was increased onto the upstream of CCL2 and CCL7 in the lung of bleomycin-treated mice, but it did not happen when EP300 was deleted in ATII cells. EP300 knockdown or inhibition suppressed the transforming growth factor beta 1 (TGF-β_1)-induced expressions of CCL2 and CCL7 in ATII cells but not club cells, fibroblast and macrophage. This study demonstrates a pivotal role for EP300 in alveolar type II cells and suggests of EP300 as a promising target for treatment of IPF.

Key words: EP300, pulmonary fibrosis, alveolar type II cell, club cell, bleomycin

The alveolar type II cell-specific functions of EP300 in pulmonary fibrosis

Soo Yeon Lee

Department of Medical Science

The Graduate School, Yonsei University

(Directed by Professor **Ho-Geun Yoon**)

I. INTRODUCTION

Idiopathic pulmonary fibrosis (IPF) is one of the most common idiopathic interstitial pneumonia and a chronic, progressive, fibrotic interstitial lung disease

of unknown cause[1]. Over time, the fibrosis gets worse and it becomes hard to take in a deep breath and the lungs cannot take in enough oxygen[2]. It is not clear what causes it, but it usually affects people who are around 70 to 75 years old, and rare in people under 50[1,2]. Many studies have attempted to elucidate the molecular mechanisms underlying pulmonary fibrosis and develop novel molecular targeted therapeutics[2]. Recently, the novel therapeutic reagents pirfenidone and nintedanib were developed to slow the progression of this complex disease[3]. However, identification and validation of more candidate therapeutic targets are still required[4].

The paradigm about IPF pathogenesis has shifted from beliefs that IPF is a result of chronic inflammation to the idea that it results from sequential injury and aberrant wound healing of the alveolar epithelium[5]. Damage to alveolar epithelium is believed to be an important early pathogenic event in IPF[5]. Under normal conditions, proliferation of alveolar type II (ATII) cells and their subsequent differentiation into alveolar type I (ATI) cells contribute to alveolar repair[6,7]. However, in IPF, both ATII cells and ATI cells die and are replaced by fibroblasts and myofibroblasts[7]. The loss of ATII cells damages the reparative mechanism and is thought to play a significant role in the development and progression of pulmonary fibrosis[6]. Indeed, ATII cells have increased expression of connective tissue growth factor (CTGF), an important mediator of pulmonary fibrosis, in

bleomycin-induced lung fibrosis, whereas blockade can abrogate fibrosis[8,9]. Additionally, a number of secreted inflammatory and profibrotic factors are released from ATII cells within the fibrotic lung[7]. Due to the suggested role of ATII cells in IPF, it is important to better understand this population to gain improved insights into disease initiation and progression[6].

It is becoming clear that IPF process is heterogeneous and many different molecular processes may be involved[2]. And recent studies show that epigenetic alterations contribute to the pathogenesis of IPF[10-12]. Accumulating evidences support the idea that epigenetic alterations, including histone acetylation, play a pivotal role in determining transcriptional profiles that contribute directly to pathogenic features of IPF[13-15]. For one, defective histone acetylation contributes for diminished COX-2 expression in IPF[15]. Therefore, there is a need for functional identification studies on key enzymes that control epigenetic changes.

Gene activation and repression are regulated of core histone[10]. Histone acetylation is mediated by coactivators that have histone acetyltransferase activity, opening up the chromatin structure to allow binding of RNA polymerase II and transcription factors[16]. This is reversed by corepressors, which include histone deacetylases and other associated corepressors that reverse this acetylation, thereby causing gene silencing[16]. In the progression of organ fibrosis, dysregulation of

histone acetylation or deacetylation is the main driving force for the development of fibrosis[12]. There are some studies of histone acetylation and deacetylation in pulmonary fibrosis[13-15]. In 2014, one study suggest that histone deacetylase inhibitors may offer a new therapeutic strategy in IPF by modulating myofibroblast susceptibility to apoptosis[13]. It was also suggests that aberrant overexpression of histone deacetylases may contribute to the fibrotic process[14]. Furthermore, it was identified that histone acetylation regulates pro-fibrotic gene expression in pulmonary fibrosis[15]. Although the necessity and importance for research about histone acetylation in pathogenesis of IPF is increasing, there is relatively little research. So, the role of histone acetyltransferase in pathogenesis of IPF has to be investigated.

Among histone acetyltransferases, E1A binding protein p300 (EP300) is the most widely studied histone acetyltransferase protein and is involved in transcriptional activation of various genes in response to cellular signaling such as inflammation, growth, and nuclear hormones[16]. It is induced by EGR1, a transcription factor of TGF-β signaling and plays an important role in regulating transcription by binding to the promoter of collagen genes, which are key genes of tissue fibrosis[17]. Recently, it has been shown that expression of active EP300 is increased in IPF patient-derived fibroblast[18]. In addition, EP300 inhibition reduces

fibrotic hallmarks of *in vitro* and *in vivo* IPF models[18,19]. These studies suggest that the control of EP300 activity may be the therapeutic target of fibrotic diseases. As shown in the case of EP300, most studies on the developmental mechanism of pulmonary fibrosis have been done in fibroblasts[17-20], but little has been done on molecular mechanisms in pulmonary epithelial cells, which are believed to have a profound connection to IPF development.

Although there are many researches that lung epithelial cells could be imortant in pathogenesis of pulmonary fibrosis, the precise mechanisms are not yet known. Having previously found evidence for epigenetic noise as an underlying cause of lung fibrosis[10,21], it was wondered whether EP300 would play a pivotal role in lung epithelial cells in the development of IPF. The research about epigenetic abnormality of lung epithelial cells could lead us to better treatment of pulmonary fibrosis.

II. Materials and methods

1. Patients samples

Human lung tissue samples were obstained from the tissue bank at Severance Hospital (Seoul, Korea). A total of 6 samples from IPF patients and control samples that is normal part of lung cancer tissue from lung cancer patients from between September 2015 and December 2016 were included in the study. The patients fulfilled the criteria of the American Thoracic Society and European respiratory Society[2] and diagnosis of IPF was supported by history, physical examination, pulmonary function studies, chest high-resolution computed tomography and corroborated by video-assisted thoracoscopic lung biopsy or transplant explants. This study was approved by the institutional review board of Severance Hospital (protocol no. 4.2016-0453).

2. Immunostaining

In preparation for immunohistochemistry, mouse lung section slides were rehydrated through a graded series of alcohols. Then, slides underwent 10 mM sodium citrate antigen retrieval. The IHC staining protocol includes sequential application of a peroxidase-blocking reagent, EP300 primary antibody (1:100,

Abcam, Cambridge, MA, USA), visualization reagent consisting of secondary antibody molecules and horseradish peroxidase coupled to a polymer backbone, 3,3'-diaminobenzidine tetrahydrochloride (DAB) chromogen reagent with hydrogen peroxide substrate (K5007, Dako, Santa Clara, CA, USA).

For immunocytochemistry, the process before binding by primary antibodies is the same as the immunohistochemistry. Primary antibodies used as follows: EP300 (1:100, sc-48343, Santa cruz Biotechnology, Dallas, TX, USA), SP-C (1:100, sc-13979, Santa cruz Biotechnology, Dallas, TX, USA), Ccsp (1:200, 07-623, Merck, Darmstadt, Germany), PDPN (1:100, AF3244, R&D, Minneapolis, MN, USA). Secondary antibodies used as follows: DyLight 488 anti-rabbit (DI-2488, Vectorlab, Burlingame, CA, USA), DyLight 549 anti-mouse (DI-1549, Vectorlab, Burlingame, CA, USA). All the Alexa Fluor coupled secondary antibodies were used at 1:500 dilutions. After staining, slides were mounted with the mounting medium with DAPI (ab104139, Abcam, Cambridge, MA, USA) and stored at 4°C in the dark. Slides were imaged and analyzed using a Zeiss LSM700 confocal microscope (Carl Zeiss, Oberkochen, Germany).

3. Animal studies

Animal experiment was approved by the Institutional Animal Care and Use Committee of Yonsei University College of Medicine (Certification No. IACUC-

2018-0087). The EP300 floxed mice and two cre mice that are used in this study were purchased from The Jackson Laboratory (Bar Harbor, ME, USA). For a conditional *Ep300* null allele, LoxP sites were inserted to flank exon 9 of *Ep300* gene[44]. The following primer sequences were used for genotyping: Ep300 5'-TGGACTGGTTATCGGTTCACC-3' and 5'-CAGTTACATACAGCTGTGATG-3'. Mice with conditional deletion of Ep300 in alveolar type II cells and club cells were generated by intercrossing $Ep300^{f/f}$ mice, Spc-CreER^{T2} and Ccsp-CreER^{T2} mice, respectively. Offspring showed expected Mendelian ratios for the predicted genotypes and both males and females EP300cKO mice were fertile. $EP300^{f/f}$ mice were used as controls in these experiments. The mice were housed with a 12 h-light/12 h-dark cycle. Before administration of bleomycin, eight-week-old mice were injected with 10 mg/kg tamoxifen (#H6278, Merck, Darmstadt, Germany) three times for one week[22]. Mice were anesthetized with an intraperitoneal injection of Zoletil 50 (30 mg/kg) and Rompun (10 mg/kg). Mice were intratracheally injected with PBS (vehicle control) or 4 mg/kg bleomycin (Santa Cruz Biotechnology, Dallas, TX, USA). The average eight mice were used for each group.

The TGF-β1-TG mice were kindly provided by a laboratory of professor Myung Hyun Sohn at Yonsei university. To induce TGF-β_1 expression, adult transgenic mice (8-12 weeks old) were placed on 0.5 mg/mL doxycycline-

containing drinking water (#D9891, Merck, Darmstadt, Germany) in 2% sucrose for four weeks[23,24]. Doxycycline-containing water was replaced three times per week.

4. Harvest and fixation of lungs

An incision was made in the abdomen and the rib cage was cut open to expose the heart and lungs. 10 mL PBS was used to perfuse the lungs through the pulmonary artery. Left lobe of mouse lung were fixed from each group in formaldehyde (4% w/v) for 48 hours at room temperature and embedded them in paraffin. Sectioning of the paraffin blocks was performed by the Histology core at the Yonsei University of Medicine at Seoul.

5. Masson's trichrome staining

To confirm collagen production by Masson's trichrome staining, sections were deparaffinized, hydrated with water. Sections were stained in Bouin's solution (#HT10132, Merck, Darmstadt, Germany) for 1 minute using microwave and then allowed to stand for 15 minutes at room temperature. After washing in running tap water, sections were placed in hematoxylin for 10 minutes, rinsed in running tap water, and stained in Biebrich scarlet for 5 minutes. Thereafter, sections were stained in phosphotungstic/phosphomolybdic acid for 15 minutes, transferred

directly into aniline blue for 5 minutes, dehydrated and coverslipped. Blue stained collagen fiber quantification was analyzed using ImageJ software in x200 field image area (Olympus, Tokyo, Japan).

6. Soluble collagen assay

Collagen content in the mouse lung tissues was determined biochemically using the Sircol Collagen Assay Kit (Biocolor, Carrickfergus, United Kingdom). In brief, lung tissues were homogenized and supernatant was collected to which collagen binding dye was added and incubated for 1 hour at 37°C, followed by centrifugation. Obtained visible red pellet was dissolved in 100% ethanol to remove excess dye and was again subjected to centrifugation. Subsequently, the pellet was dissolved in 0.5 M sodium chloride solution, incubated for 30 minutes at 37°C and absorbance was measured at 540 nm using spectrophotometer.

7. Cell culture and reagents

Rat lung alveolar type 2 cell line RLE-6TN, mouse lung club cell line C22, mouse fibroblast cell line Mlg and mouse lung alveolar macrophage cell line MH-S were purchased from Korean Cell line Bank (Seoul, Korea). RLE-6TN and MH-S were cultured in Dulbecco's modified Eagle's medium supplemented with 10% (v/v) fetal bovine serum and 1% antibiotic/antimycotic solution (Corning,

Manassas, VA, USA) at 37ºC under 5% CO_2. MH-S were grown in complete DMEM supplemented with 50 μM 2-mercatoethanol. C22 were maintained in permissive conditions [DMEM supplemented with 4% FBS, penicillin (100 U/ml), streptomycin (100 μg/ml), 2 mM glutamine, endothelin-1 (0.25 μg/ml), interferon-γ (0.01 μg/ml), insulin (10 μg/ml), transferrin (5 μg/ml), endothelial cell growth supplement (7.5 μg/ml), epidermal growth factor (0.025 μg/ml), hydrocortisone (0.36 μg/ml), and T_3 (0.02 μg/ml)] at 33 °C under 5% CO_2. Bleomycin was purchased from Santa Cruz Biotechnology (Dallas, TX, USA). C646 was purchased from Sigma-Aldrich (St. Louis, MO, USA). TGF-β1 was purchased from ProSpec (East Brunswick, NJ, USA).

8. Construction of stable transfected cell lines

To generate the cell lines for stable knockdown of *EP300*, lentiviral vectors (scramble, shep300) used in this study were purchased from Sigma-Aldrich, U.S.A. The auxiliary plasmid liposomes (pxPAX.2 and Pmd2.G) and lentivirus vector were transfected into 293FT cells to produce lentivirus by using Lipofectamine 3000 transfection reagent (Invitrogen, Carlsbad, CA, USA). After 48 hours of transfection, the supernatant was collected and centrifuged to discard cell debris. The centrifuged supernatant was filtered by using a 0.45 μm polyvinylidene difluoride filter. RLE-6TN, C22, MH-S and MLg cells were infected with viral

suspension mixed with 8 μg/ml polybrene. After 48 hours of infection, 2 μg/ml puromycin was added to screen the positive stably transduced cell lines.

9. RNA isolation and quantitative reverse transcription-polymerase chain reaction (qRT-PCR)

Total RNA was extracted using TRIzol reagent following the standard protocol (Takara, Kyoto, Japan) and cDNA was synthesized using CellScript (CellSafe, Seoul, Korea), following to the manufacturer's protocol. The concentration of cDNA was normalized using GAPDH. Quantitative RT-PCR analyses was performed using SYBR Green PCR master mix reagents and an ABI Prism 7700 sequence detection system (Applied Biosystems, Carlsbad, CA, USA). All reactions were performed in triplicate. Relative expression levels and standard deviations of target genes were calculated using the comparative method. qRT-PCR was performed using the following forward and reverse primers:

rat Gapdh, forward: 5'- TGATTCTACCCACGGCAAGTT-3' and reverse: 5'-TGATGGGTTTCCCATTGATGA-3';

rat Ccl2 forward: 5'- CAGATGCAGTTAACGCCCCA-3' and reverse: 5'-TTGAGCTTGGTGACAAAAACTACAG-3';

rat Ccl7, forward: 5'- GCACCGAGTCTGCCAACTTT-3' and reverse: 5'-

GGATGAATTGGTCCCATCTGGT-3';

mouse Gapdh forward; 5'- CGACTTCAACAGCAACTCCCACTCTTCC-3' and reverse: 5'- TGGGTGGTCCAGGGTTTCTTACTCCTT -3'

mouse Ccl2 forward: 5'- CAGATGCAGTTAACGCCCCA-3' and reverse 5'- TTGAGCTTGGTGACAAAAACTACAG-3'

mouse Ccl7 forward: 5'- GAGTCTGCCAGCTCTCACTG-3' and reverse 5'- GCATTGGGCCCATCTGGTTG-3'

10. Isolation of primary alveolar II cells

For RNA-seq analysis, primary murine alveolar type II cells were obtained from 8-10 weeks old C57BL/6 and alveolar type II cell-specific Ep300 KO mice. Mice were sacrificed and the lungs perfused and cannulated as described above. 2mL dispase (1 U/mL, #07923, Stemcell, Vancouver, Canada) was instilled into the lungs to seal the upper airway. The lungs were removed and incubated in dispase. at room temperature for 40 minutes. After enzymatic digestion with dispase, lung tissue was gently minced with a GentleMACS DIssociator (Miltenyi Biotec, Bergisch Gladbach, Germany). Cells were first incubated with red blood lysis buffer. After spinning down, cells were blocked in. Cells were then stained with different antibodies. Antibodies used: Ep-CAM-APC (1:100, #17-5791-82, Invitrogen,

Waltham, MA, USA), CD74-FITC (1:100, #555318, BD Biosciences, San Jose, CA, USA). Sorting was performed on a BD FACSAria™ III flow cytometer (BD Biosceinces, San Jose, CA). One mouse was used for each isolation; the typical yield was ~1.0×10^6 primary ATII cells per animal. Cell purity was determined via immunocytochemical staining of samples using SFTPC to label primary ATII cells.

11. RNA-sequencing

Total RNA was isolated using Trizol reagent (Invitrogen, Waltham, MA, USA). RNA quality was assessed by Agilent 2100 bioanalyzer using the RNA 6000 Nano Chip (Agilent Technologies, Amstelveen, Netherlands), and RNA quantification was performed using ND-2000 Spectrophotometer (Thermo Fisher Scientific, Waltham, MA, USA).

For control and test RNAs, the construction of library was performed using QuantSeq 3'mRNA-Seq Library Prep Kit (Lexogen BioCenter, Vienna, Austria) according to the manufacturer's instructions. In brief, each 500ng total RNA were prepared and an oligo-dT primer containing an Illumina-compatible sequence at its 5'end was hybridized to the RNA and reverse transcription was performed. After degradation of the RNA template, second strand synthesis was initiated by a random primer containing an Illumina-compatible linker sequence at its 5'end. The double-stranded library was purified by using magnetic beads to remove all reaction

components. The library was amplified to add the complete adapter sequences required for cluster generation. The finished library is purified from PCR components. High-throughput sequencing was performed as single-end 75 sequencing using NextSeq 500 (Illumina, San Diego, CA, USA).

12. ChIP-sequencing

Whole lungs of bleomycin- and PBS-treated mouse were used for ChIP-seq analysis, which were performed by Active Motif (Carlsbad, CA, USA). The samples were fixed and subjected to immunoprecipitation using an antibody against Ep300. In brief, the 75-nt single-end (SE75) sequence reads generated by Illumina sequencing (using NextSeq 500) are mapped to the genome using the BWA algorithm with default settings. Reads were extended at their 3'-ends to a length of 200 base pair fragments in a size-selected library. The densities of fragments (signal map) were determined by the number of fragments in each 32-nt bins along genome. The tag number of samples within a comparison group was normalized by random sampling to the number of tags in the smallest sample. Data was visualized by the University of California, Santa Cruz (UCSC) genome browser. Enrichr[25] were used for pathway analysis.

13. Statistical Analysis

All results were analyzed with Prism software, version 5 (GraphPad Software, San Diego, CA, USA) and are shown as the mean±standard error of the mean. Student's *t*-test used for determining statistical significance of two groups. The significance levels are indicated as follows: not significant, $P>.5$; *, $P\leq.05$; **, $P\leq.01$; and ***$P\leq.001$.

III. RESULTS

1. Expression of EP300 is elevated in the lungs of patients with IPF and in mouse models of lung fibrosis

Recent studies show that EP300 has profibrotic activity and EP300 inhibition attenuates pulmonary fibrosis[17-19,26]. These findings suggest EP300 may play an important role in lung fibrosis. To examine the roles of EP300 in lung epithelial cells, the levels of EP300 were assessed in lung tissues of IPF patients and mouse models of lung fibrosis. Immunochemistry staining showed that EP300 was significantly increased in samples from IPF patients compared to those from control subjects (Figure 1A-B). Bleomycin (BLM) is widely used for acute induction of lung fibrosis in mice and TGF-β_1 levels which is potent fibrogenic cytokine that plays a critical role in IPF pathogenesis[27]. EP300 levels were significantly increased in the lungs of mice following bleomycin injection (Figure 1C-D).

To examine the cell type-specific expression of EP300 in the lung tissues from bleomycin-induced mice, co-IF staining was performed using antibodies for Pro-SPC (ATII cell marker), CCSP (club cell marker), Muc5AC (goblet cell marker), Foxj1 (ciliated cell marker) and α-SMA (fibroblast marker). The expression of EP300 was significantly increased by BLM injection in both ATII cell and club cell,

but not goblet cell, ciliated cell, and fibroblast (Figure 1E-F). These results demonstrate that EP300 expression increases in IPF and lung epithelial cells of lung fibrosis mouse model.

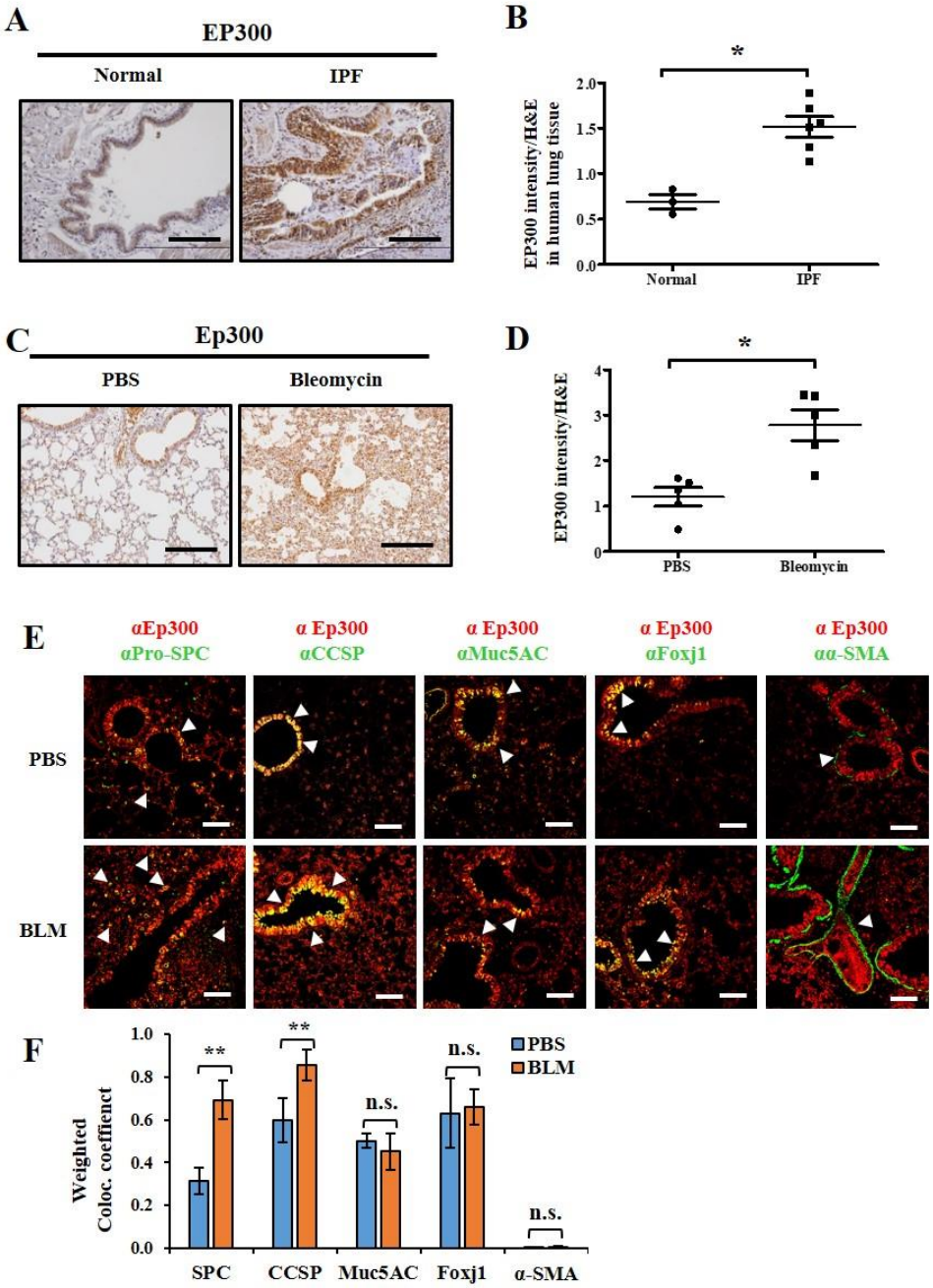

Figure 1. Elevated expression of EP300 in IPF patients and in a mouse lung fibrosis model. (A) Immunohistochemistry staining with anti-EP300 antibody was performed in normal lung (n=5) and IPF lung (n=5) specimens. (B) Dot plot represents EP300 intensity/H&E ratio from IPF patients (n=3) and the control subjects (n=6). IPF vs. control; 1.5 (1.1-1.8) vs. 0.7 (0.5-0.9), p=0.0204. (C) Immunohistochemistry in lung sections from normal and bleomycin-induced fibrotic mice. (D) EP300 and H&E intensities in bleomycin-induced lung fibrosis mice (n=5) and control (n=5) were analyzed using ImageJ software. PBS vs. bleomycin; 1.2 (0.4-1.6) vs. 2.7 (1.6-3.4), p=0.0339. (E) Co-Immunofluorescence assay was carried out with mouse lung tissues using indicated antibodies. Pro-SPC is an AT2 cell marker; CCSP is a club cell marker; Muc5AC is a goblet cell marker; α-SMA is a fibroblast marker; Foxj1 is a ciliated cell marker. Localization of EP300 (red staining) was incubated with EP300 mouse monoclonal antibody and visualized using DyLight 549 anti-mouse antibody. These same cells were incubated with each cell marker antibodies and visualized (green staining) using DyLight 488 anti-rabbit antibody. Colocalization of EP300 and each cell marker was determined by merging individual red and green images to give orange-labelled cells. Co-localized EP300 and each marker is indicated by white arrowheads. Scale bar = 50 um. (F) Weighted co-localized coefficient was calculated using ZEN 2.3

software. All IHC images are magnification ×200. Scale bars of IHC images, 100μm. BLM; bleomycin.

2. Lung fibrosis is regulated by EP300 in an alveolar type II cell-specific manner

Based on IHC analysis of EP300 in in lung tissues of IPF patients and mouse models of lung fibrosis, the majority of EP300 were observed in the area of bronchiolar epithelium and alveolar region. To elucidate the role of EP300 on the development of lung fibrosis in alveolar type II cells, a genetically engineered mouse model with tamoxifen-inducible Ep300 ablation in ATII cells (*Spc-Ep300*$^{d/d}$) was generated. To determine the role of ATII cell-specific Ep300 in the bleomycin-induced acute lung inflammatory response, bleomycin was administered both to *Ep300*$^{f/f}$ mice and *Spc-Ep300*$^{d/d}$ mice. It was observed bleomycin-induced lung fibrosis was markedly inhibited in *Spc-Ep300*$^{d/d}$ mice by using Masson's trichrome staining (Figure 2A and B). To quantify the amount of collagen deposition, the lungs were analyzed for soluble collagen content via Sircol collagen assay. Deletion of Ep300 in ATII cells prevents bleomycin-induced accumulation of collagen compared to control mice (Figure 2C). In addition, total cells of BAL Fluid and body weight loss were reduced in bleomycin-treated *Spc-Ep300*$^{d/d}$ mice compared to PBS-treated mice (Figure 2D and E). Taken together, these data suggest that ATII cell-specific EP300 plays important role in lung fibrosis progression.

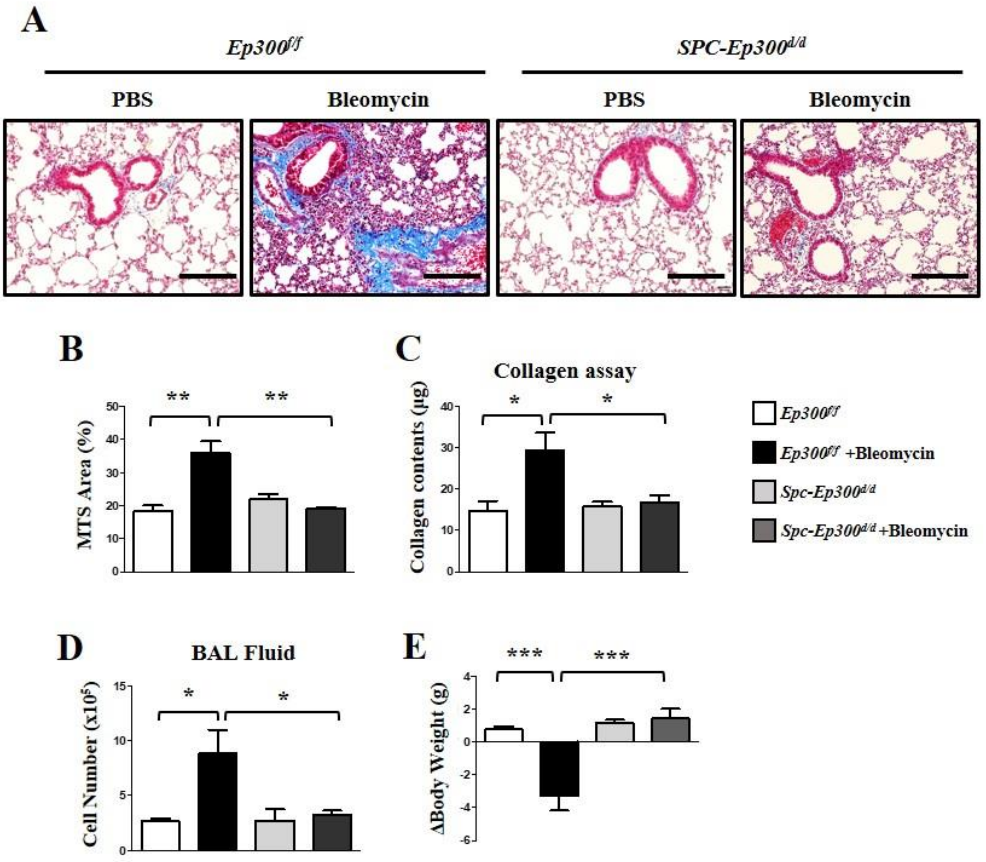

Figure 2. ATII cell-specific deletion of *Ep300* prevents lung fibrosis. The *Ep300*$^{f/f}$ and *Spc-Ep300*$^{d/d}$ mice were treated with 4 mg/kg of bleomycin and sacrificed 14-days post injection. (A) Representative images of Masson's trichrome stained lung sections of *Ep300*$^{f/f}$ and *Spc-Ep300*$^{d/d}$ mice. (B) Quantification of collagen area of Masson's trichrome staining. (C) Assessment of lung collagen content using Sircol Collagen assay at day 14. (D) Total cell count from the BAL Fluid of *Spc-Ep300*$^{d/d}$ and control mice at day 14. (E) Change in body weight of

mice treated with bleomycin and control mice (n=9/group). Survival curves were presented as a Kaplan-Meier plot. Statistical analysis was performed by Student's t test: *$p < 0.05$, **$p < 0.01$, and ***$p < 0.005$.

3. Club cell-specific EP300 knockout does not affect lung fibrosis following bleomycin exposure

Next, to determine the physiological role of EP300 on lung fibrosis in club cells, a genetically engineered mouse model in which Ep300 is specifically ablated in club cells was generated. Mice expressing Cre recombinase from the club cell secretory protein (CCSP) promoter were crossed with Ep300 floxed mice (*Ccsp-Ep300*$^{d/d}$). In contrast to *Spc-Ep300*$^{d/d}$ mice, there were no significant changes related to fibrosis in *Ccsp-Ep300*$^{d/d}$ mice (Figure 3A and B). In the lung tissue, bleomycin injection resulted in increasing soluble collagens, with no apparent differences between control and *Ccsp-Ep300*$^{d/d}$ mice. The total cell number of BAL Fluid and body weight loss were similar between control and *Ccsp-Ep300*$^{d/d}$ mice (Figure 3D and E). Therefore, ablation of Ep300 gene in club cells had no effect in the bleomycin-induced lung fibrosis.

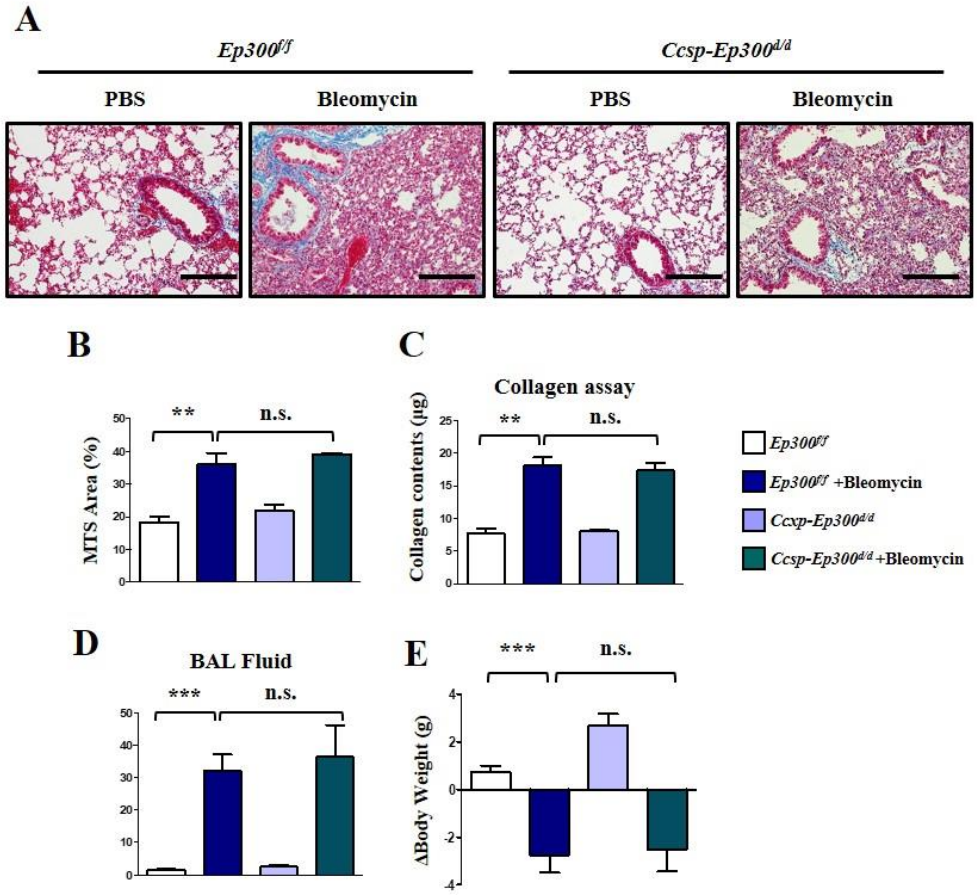

Figure 3. Club cell-specific deletion of *Ep300* has no effect on bleomycin-induced lung fibrosis. The *Ep300*$^{f/f}$ and *Ccsp-Ep300*$^{d/d}$ mice were treated with 4 mg/kg of bleomycin and sacrificed 14-days post exposure. (A) Representative images of Masson's trichrome stained lung sections of *Ep300*$^{f/f}$ and *Ccsp-Ep300*$^{d/d}$ mice. (B) Quantification of collagen area of Masson's trichrome staining. (C) Assessment of lung collagen content using Sircol Collagen assay at day 14. (D) Total cell count from the BAL Fluid of *Ccsp-Ep300*$^{d/d}$ and control mice at day 14.

(E) Change in body weight of mice treated with *Ccsp-Ep300*$^{d/d}$ and control mice (n=9/group). Survival curves were presented as a Kaplan-Meier plot. Statistical analysis was performed by Student's t test: *$p < 0.05$, **$p < 0.01$, and ***$p < 0.005$.

4. Ablation of Ep300 in alveolar type II cells prevents progression of established TGF-β-induced pulmonary fibrosis

To further validate the selective role of EP300 in the development of lung fibrosis, a transgenic mouse model with inducible overexpression of TGF-β_1 (*Ccsp-TGFβ_1*-TG mice)[24], which induces lung fibrosis after administration of doxycycline (Dox), was adapted for this experiment. The mice were placed on 0.5 mg/mL doxycycline-containing drinking water supply for 4 weeks. During doxycycline administration, additional intraperitoneal administration of tamoxifen was injected once a week (Figure 4A). After 28 days of Dox, EP300 was significantly increased in the lungs of *Ccsp-TGFβ_1*-TG mice compare to lungs from wild-type mice (Figure 4B), however, previously observed increased lung fibrosis was significantly reduced in *Spc-Ep300$^{d/d}$*/*Ccsp-TGFβ_1*-TG mice(Figure 4B and C). ATII cell-specific Ep300 knockout inhibited accumulation of collagen (Figure 4D) and decreased total cell number of BAL Fluid (Figure 4E). Taken together, this data corroborates our finding that Ep300 mediates lung fibrosis in ATII cell-specific way.

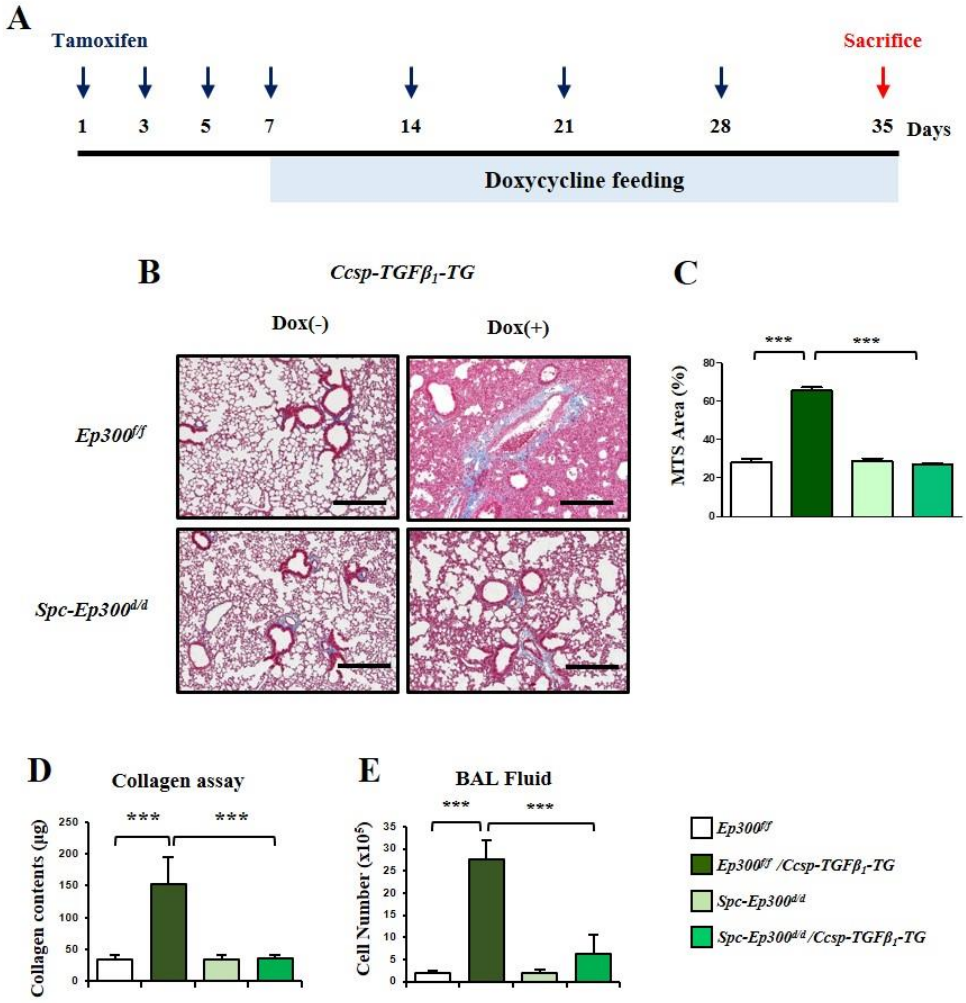

Figure 4. Ablation of *Ep300* in alveolar type II cells inhibits in *CCSP-TGFβ1*-TG mice. (A) Scheme for doxycycline treatment to generate epithelial *Ccsp-TGFβ1*-TG mice with tamoxifen injection. Mice were treated with doxycycline-containing water for 4 weeks. (B) Masson's trichrome staining of lungs of *Spc-Ep300$^{d/d}$/Ccsp-TGFβ1*-TG and control mice. (C) Quantification of collagen fiber of

Masson's trichrome staining. (D) Lung collagen content in lung obtained from *Spc-Ep300$^{d/d}$/Ccsp-TGFβ$_1$*-TG and control mice. Changes in collagen content in right lung homogenate samples measured by Sircol Collagen assay. (E) Total cell count of BAL Fluid of *Spc-Ep300$^{d/d}$/Ccsp-TGFβ$_1$*-TG and control mice at day 14. Statistical analysis was performed by Student's t test: *$p < 0.05$, **$p < 0.01$, and ***$p < 0.005$;

5. Ep300 regulates the expression of the genes related to extracellular matrix and chemokines in murine primary ATII cells

To determine whether EP300 is involved in transcriptional regulation of TGF-β target genes, RNA-sequencing analysis was performed using murine primary ATII cells. ATII cells were isolated from the lungs of four groups: (PBS-treated *Ep300*$^{fl/fl}$ mice (WT), bleomycin-treated *Ep300*$^{fl/fl}$ mice (BLM), PBS-treated *Spc-Ep300*$^{d/d}$ mice (KO), bleomycin-treated *Spc-Ep300*$^{d/d}$ mice (KO-BLM)). To isolate primary ATII cells, flow cytometric analysis was performed for double-staining using the antibodies against Ep-Cam and Cd74, which are the surface markers of ATII cells (Figure 5A). Gene set enrichment analysis (GSEA) demonstrated significant enrichment of extracellular matrix and chemokine genes in ATII cells of BLM mice (Figure 5B). However, Ep300 knockout negatively regulated extracellular matrix and chemokine Gene Ontology (GO)-defined genes (Figure 5C). The RNA-sequencing data showed 2,834 genes in ATII cells of BLM mice were significantly changed compared to WT mice (Fold change > 2.0, p-value < 0.05). Among them, 1,588 genes were significantly upregulated and 741 genes were downregulated. Of the upregulated genes, 700 genes were reduced when Ep300 was ablated in ATII cells. They were arranged by heatmap (Figure 5D) and top 30 genes were indicated. Most of them were the genes involved in extracellular matrix or chemokines.

Therefore, these data suggest that Ep300 regulates the gene expressions of extracellular matrix and chemokines in ATII cells.

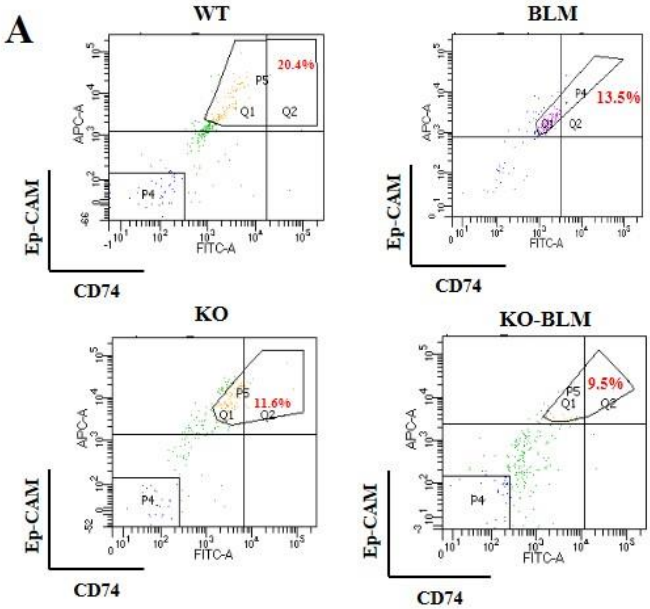

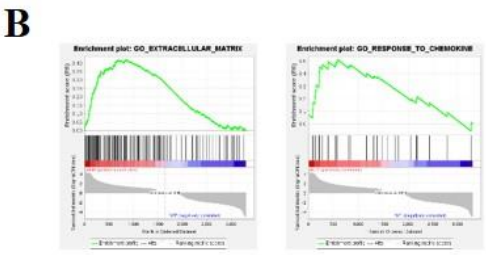

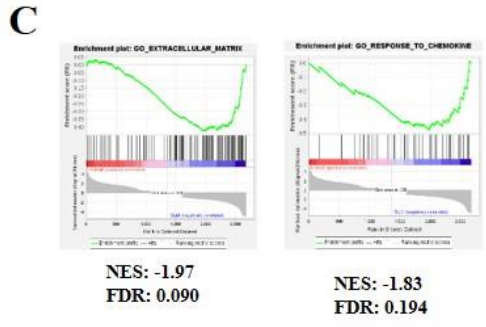

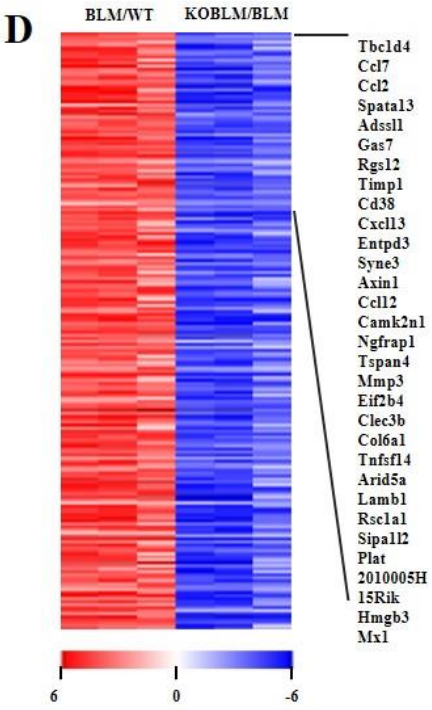

Figure 5. EP300 mediates TGF-β-dependent transcriptional activation of extracellular matrix and chemokine genes. (A) Isolation of ATII cells from control (WT), bleomycin-treated (BLM), *Spc-Ep300*$^{d/d}$ (KO) and bleomycin-treated *Spc-Ep300*$^{d/d}$ (KO-BLM) mice. FACS plots showing the sequential gating strategy used to isolate ATII cells. (B) GSEA enrichment plots of 'Extracellular Matrix' (left) and 'Response to Chemokine' (right) gene sets from analysis comparing WT mice and BLM mice samples. (C) GSEA enrichment plots of 'Extracellular Matrix' (left) and 'Response to Chemokine' (right) genes sets from analysis comparing BLM mice and KO-BLM mice samples. (D) A heatmap of extracellular matrix and chemokine gene signature is pictured. Red, positive log fold-change (logFC) indicates higher expression in the genes from ATII cells of BLM mice compared with WT mice. Blue, negative logFC indicates lower expression in genes from ATII cells of KO-BLM mice compared with BLM mice. Top 30 selected genes from two comparisons are indicated. (log fold-change>2.0, p-value<0.05) NES, normalized enrichment score; FDR, false discovery rate.

6. EP300 directly regulates transcription of Ccl2 and Ccl7 chemokine genes in ATII cells

EP300 functions as a histone acetyltransferase that regulates transcription of genes via chromain remodeling[42]. To identify direct target genes of Ep300, chromatin immunoprecipitation sequencing (ChIP-sequencing) in bleomycin-induced fibrosis and control lung was performed. ChIP-sequencing analysis identified 2,066 significant peaks (693 upregulated and 1,373 downregulated) for EP300 binding sites in fibrotic lung. Pathway analysis using EnrichR[29] identified significant enrichment of biological processes related to macrophage and neutrophil activation, immune responses (Figure 6A). By comparing the ChIP-sequencing and RNA-sequencing results, 72 genes were identified, which not only contain EP300-binding sites (Figure 6B), but whose expression was altered in the ATII cells of *Spc-Ep300*$^{d/d}$ mice with bleomycin treatment as compared to *Ep300*$^{f/f}$ mice. Ccl2 and Ccl7 were down-regulated in the ATII cells of *Spc-Ep300*$^{d/d}$ mice with bleomycin treatment and include up-regulated Ep300-binding site. The recruitment of EP300 onto Ccl2 and Ccl7 genes in fibrotic lung was confirmed by ChIP-sequencing analysis (Figure 6C). Collectively, these results suggest that Ccl2 and Ccl7 are putative target genes of Ep300 in the development of lung fibrosis.

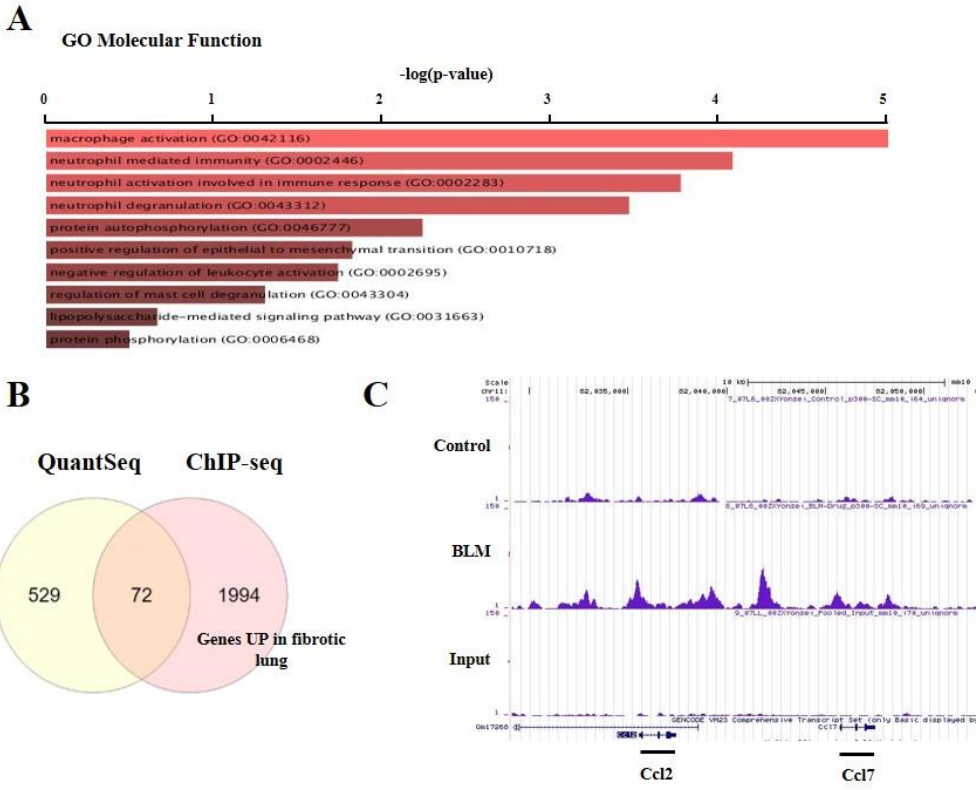

Figure 6. Chromatin immunoprecipitation-sequencing analysis (ChIP-sequencing) of whole lung tissue from normal and fibrotic lung. ChIP-sequencing analysis of genomic locations of DNA fragments immunoprecipitated by Ep300 antibody in whole lungs of bleomycin- or PBS- treated mice. (A) Gene ontology analysis of significantly upregulated genes in fibrotic lung tissues more than normal. Gene lists were generated using a cut-off of positive and negative fold change >1.5 and adjusted p-value of <0.05. (B) Venn diagrams show overlapping of the genes between ChIP-sequencing showing gain of Ep300 and RNA-

sequencing showing significant differentially upregulated or downregulated genes. (C) Representative peaks for Ep300 binding sites at the genes Ccl2, Ccl7 in normal and fibrotic lungs compared to input control.

7. The binding of EP300 on promoter regions of CCL2 and CCL7 increases in lungs of bleomycin-treated mice

To determine EP300 actually binds to the sites from ChIP-sequencing results, ChIP assay was performed using mouse lung tissue. There were putative sites where EP300 was expected to bind onto the upstream of each gene (Figure 7A). For CCL2 gene, the binding of EP300 in #2 (-30,662), #3 (-28,663) and #6 (-12,827) of the seven sites was increased in the lungs of mice treated with bleomycin (Figure 7B). However, the recruitment of EP300 to three binding sties of CCL2 was fully abolished by *EP300* ablation. In addition, the bindings of EP300 to the other sites of CCL2 gene were not observed by BLM injection.

For CCL7 gene, there were three putative sites where EP300 was expected to bind. It was observed that the binding of EP300 to #1 (-3773) of CCL7 gene was increased by bleomycin treatment compared to control (Figure 7C); however, the binding of EP300 to #1 of CCL7 was completely abolished by ATII cell-specific *EP300* deletion. Moreover, the bindings of EP300 to the other sites (#2 and #3) of CCL7 gene were not observed by BLM injection. These data demonstrate that the EP300 binds to upstream of CCL2 and CCL7 upon induction of pulmonary fibrosis.

A

Gene	No.	Distance to Start	Position	Increased binding of Ep300
CCL2	#1	-38,404	upstream	×
	#2	-30,662		○
	#3	-28,663		○
	#4	-20,367		×
	#5	-19,117		×
	#6	-12,827		○
	#7	-11,717		×
CCL7	#1	-3,773	upstream	○
	#2	-10,268		×
	#3	-6,586		×

B

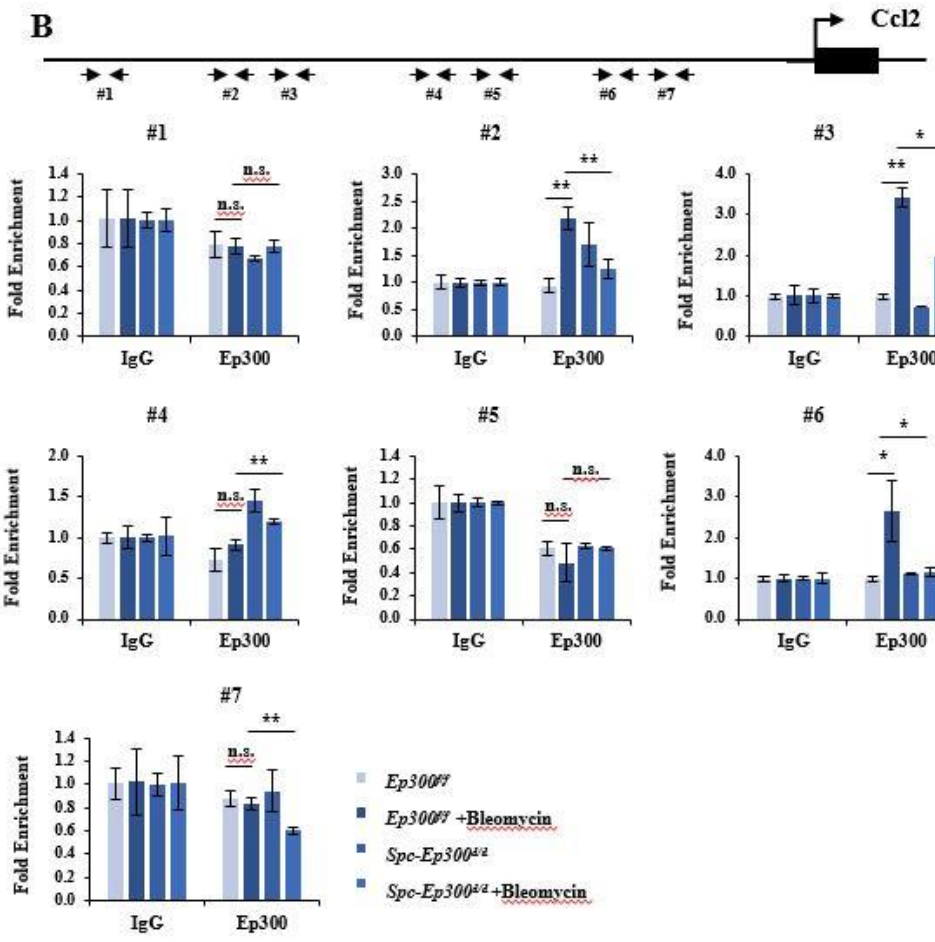

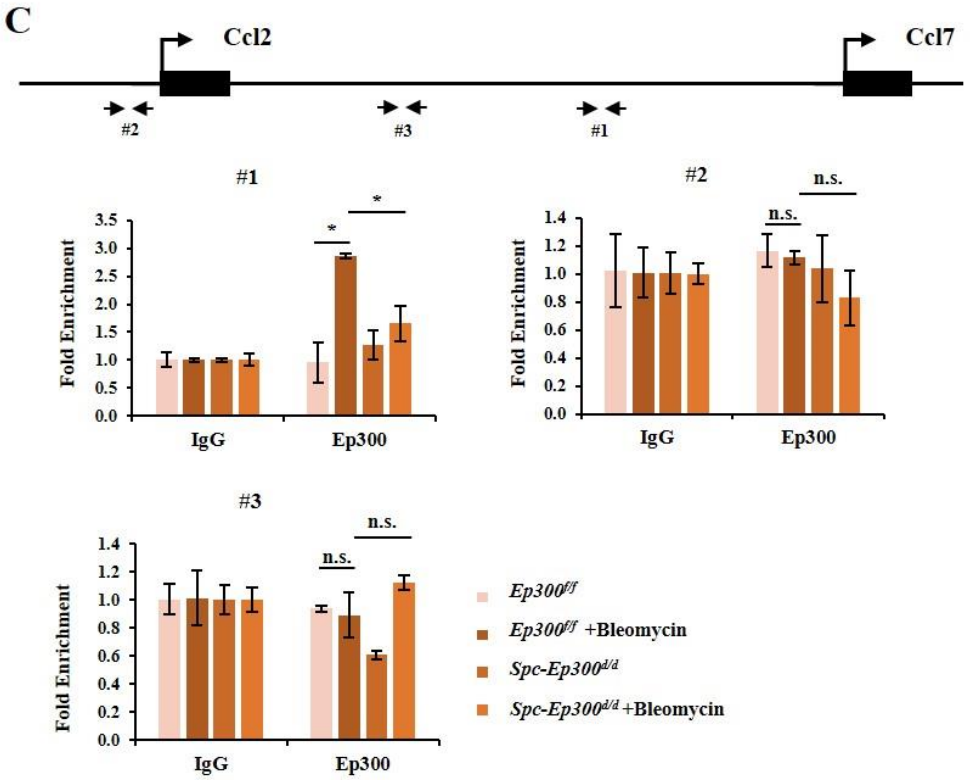

Figure 7. Chromatin immunoprecipitation (ChIP) analysis of EP300 within the promoter regions of CCL2 and CCL7 after PBS or bleomycin treatment of *Ep300$^{f/f}$* and *Spc-Ep300$^{d/d}$* mice. (A) A table showing EP300 binding sites in the upstream regions of CCL2 and CCL7 from the results of ChIP-sequencing. Lung tissue derived from *Ep300$^{f/f}$* and *Spc-Ep300$^{d/d}$* mice that injected by PBS or bleomycin were subjected to ChIP analysis to examine EP300 within the promoter regions of CCL2 and CCL7. They were numbered in the order of distance from the gene (CCL2) or high log values of ChIP-sequencing results (CCL7). (B) Chromatin

immunoprecipitation (ChIP) analysis of EP300 within the 7 upstream sites of CCL2 that are expected to bind EP300. Lung tissue derived from *Ep300*$^{f/f}$ and *Spc-Ep300*$^{d/d}$ mice that received PBS or bleomycin (4 mg/kg) were subjected to ChIP analysis. (C) Chromatin immunoprecipitation (ChIP) analysis of EP300 within the 3 upstream sites of CCL7 that are expected to bind EP300. Arrows indicate the location of the quantitative polymerase chain reaction primer binding within upstream regions of CCL2 and CCL7. The results are expressed as a the mean±SEM fold change (n=3/group). *, $p < 0.05$; **, $p < 0.01$; ***, $p < 0.001$; N.S., not significant.

8. Downregulation of Ccl2 and Ccl7 by Ep300 inhibition is significant in alveolar type II cells rather than other cells

To verify the selective action of EP300 in the transcriptional regulation of both CCL2 and CCL7 genes, the qRT-PCR were performed in RLE-6TN (rat ATII cell), C22 (mouse club cell), MLg (mouse fibroblast) and MH-S (mouse macrophage). The TGF-β_1-induced expression of Ccl2 and Ccl7 was observed in RLE-6TN, MLg and MH-S, but not in C22. TGF-β_1-induced expression of Ccl2 and Ccl7 were significantly down-regulated by Ep300 knockdown or inhibition in ATII cells (Figure 8A). However, Ep300 knockdown or inhibition had no effects on the mRNA levels of Ccl2 and Ccl7 in C22, MLg and MH-S cells (Figure 8B-D). These results suggest that Ep300 selectively regulates TGF-β_1-induced transcriptional activation of Ccl2 and Ccl7 genes in ATII cell.

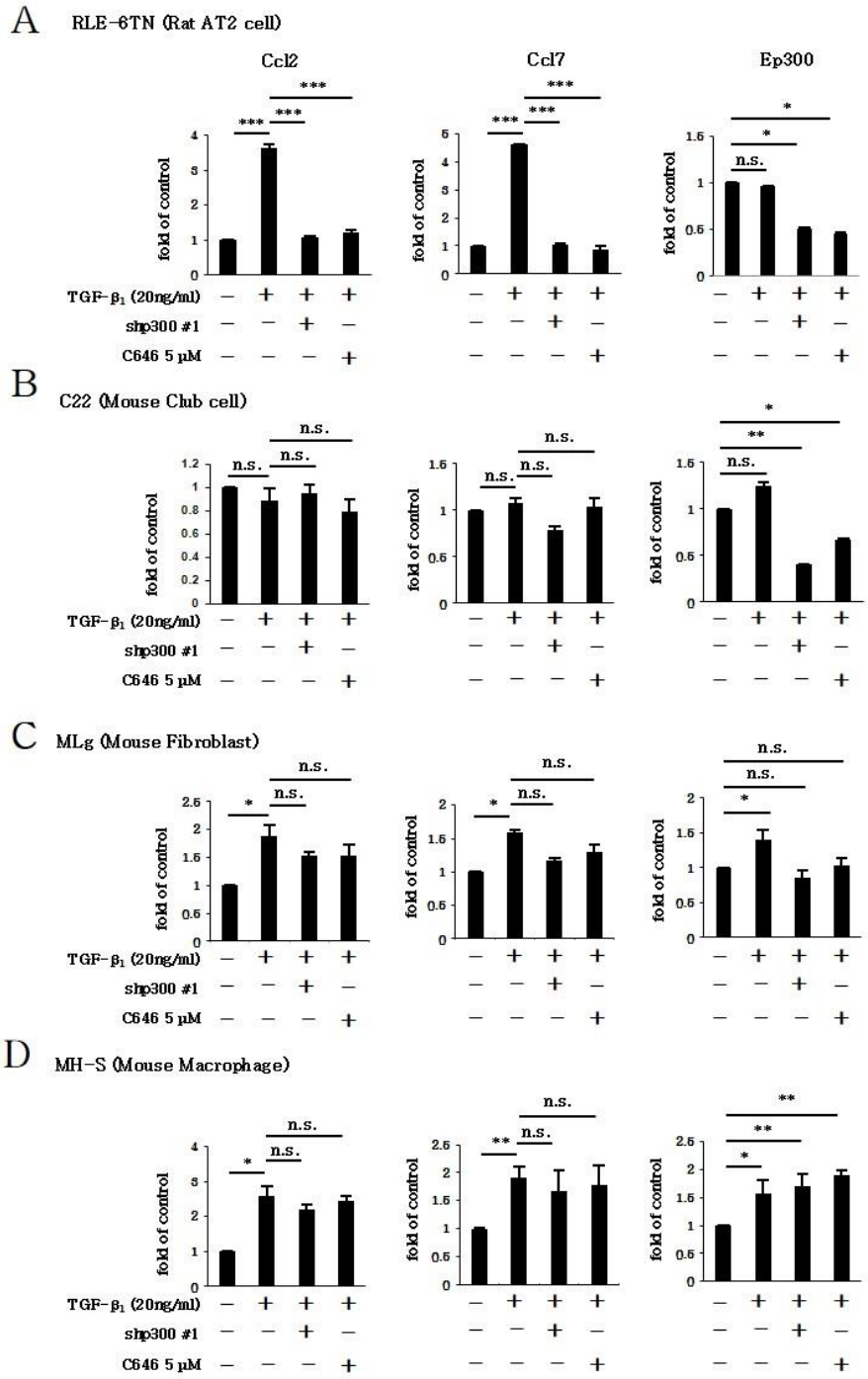

Figure 8. Ep300 knockdown or inhibition reduced the mRNA expression level of Ccl2 and Ccl7 in alveolar type II cells. (A-D) qRT-PCR analysis of expression of Ccl2 and Ccl7 genes in lung cells. The cells were serum-starved for 2 hours before TGF-β_1 (20 ng/mL) treatment and pretreated with 5 μM C646, which is one of the Ep300 inhibitors, when serum-starvation was initiated. Cells were harvested after 24 hours of TGF-β_1 treatment. Statistical analysis was performed by Student's t test: Error bars, SD (n = 3); *, $p < 0.05$; **, $p < 0.01$; ***, $p < 0.001$; N.S., not significant.

IV. DISCUSSION

IPF is a fatal interstitial lung disease for which no cure exists[1]. Although two drugs have been approved for the treatment of IPF in several contries[3], the survival of IPF patients remains poor. IPF is initiated by inflammation followed by a massive production of fibrous connective tissue in the interalveolar septa[4]. This fibrotic process results in an excessive number of fibroblasts, an increase in lung collagen content, abnormal spatial distribution of extracellular matrix proteins and, ultimately, deteriorated lung function[1]. However, the molecular mechanisms responsible for the inflammatory process and the ensuing fibrotic alternations in IPF are not well understood. Thus, the search for IPF continues and to find out the mechanism of IPF is important.

Much of the research into the pathogenesis of fibrosis in the past few decades has focused on the function of fibroblasts and myofibroblasts. Fibroblasts and myofibroblasts accumulate in fibroblastic foci that, as the predominant sites of excess matrix production, can be thought of as the leading edge of active fibrosis[28]. Activation and accumulation of fibroblasts in IPF, however, appears to be fundamentally driven by recurrent and non-resolving injury to the alveolar epithelium, and therefore in another sense, the injured alveolar epithelium can be

thought of as the leading edge of active fibrosis[29]. With fibroblasts and alveolar epithelial cells being in close apposition in the lung, it is not surprising that the effects of these two key cellular players contribute to the development of pulmonary fibrosis. Although the role of epithelial cells is as important as fibroblasts in the pathogenesis of lung fibrosis, there is not enough research on it. This study demonstrates that EP300 plays a pivotal role in ATII cells of fibrotic lungs for the first time.

Respiratory epithelium is comprised of a diverse and dynamic population of cells which are abundant in the lung and can respond to various stimuli with dramatic phenotypic changes that are critical for the initiation and progression of fibrosis[30]. Extensive evidence from human tissue and animal models suggest that epithelial cell apoptosis occurs and is sufficient for initiating robust fibrosis[31]. This may be partially through a failure of the epithelial cells to regenerate the damaged epithelium and restore the anti-fibrotic homeostatic environment, as well as through an active initiation of a pro-fibrotic program by the dying epithelial cells[31]. After diverse injuries, epithelial cells can become activated in ways that overlap with the traditional pro-fibrotic functions of activated fibroblasts including generation of pro-fibrotic cytokines and deposition of fibrotic matrix proteins[30]. In this study, EP300 was upregulated in the epithelial cells of bleomycin-induced mice, not in

fibroblasts. It suggests that EP300 could play a crucial role in epithelial cells for pathogenesis of lung fibrosis. In situations other than the model used in this study, the responses in fibroblast may be different, so further studies are required.

Recently, there are increasing evidences that among lung epithelial cells, alveolar type II (ATII) cells could be a driver of IPF and have a central role in pulmonary fibrosis[6]. ATII cells are a heterogeneous population that have critical secretory and regenerative roles in the alveolus to maintain lung homeostasis[7]. However, impairment to their normal functional capacity and development of a pro-fibrotic phenotype has been demonstrated to contribute to the development of lung fibrosis[6]. ATII cells are also exposed to environmental stresses that can have lasting effects that contribute to fibrogenesis[32]. Furthermore, it was identified that genetic risks can cause ATII cells impairment and the development of lung fibrosis[6,7]. So, understanding the role of ATII cells in pulmonary fibrosis is essential for the treatment of IPF. In accordance with the current, this study demonstrated that genetic deletion of EP300 in AT2 cells, but not clara cells, abrogates BLM and TGF-β-induced lung fibrosis, indicating a selective action of EP300 in AT2 cells. This study lays the groundwork towards more efficient way targeting EP300 of ATII cells in IPF.

As well as alveolar type II cells in the alveolar compartment, other epithelial

cell types populate the lung; with secretory Clara and goblet cells, ciliated, basal and neuroendocrine cells. According to recent studies, club cells have cellular and molecular heterogeneities[30]. Depending on its type, it appears to have a different effect on the pathogenesis of lung fibrosis[33]. In addition, inhibition of lung fibrosis in club cell-depleted lung implies that club cell is involved in pathogenesis of the disease and plays a role of progenitor cells[34]. These data reveal that EP300 deletion in club cell did not affect the pathogenesis of lung fibrosis. Transcriptional expression of CCL2, CCL7 and CCL12 were not induced by TGF-β1 in club cell and were also not affected by knockdown or inhibition of EP300. Therefore, it is thought that EP300 plays a different role in the club cells than ATII cells.

Pulmonary fibrotic diseases are often associated with arrest of monocytes, neutrophils, mast cells and other leukocytes[2]. The release of chemokines by these pro-inflammatory cells and also by resident cells (alveolar epithelial cells) enhance the inflammatory and fibrotic effects in the lung[35]. Among chemokines, CCL2 is the most extensively studied chemokine in lung fibrosis[36]. Elevated CCL2 has been found in BAL fluid and serum samples from IPF patients[37,38]. Moreover, alveolar epithelial cells within fibrotic areas were reported to have augmented CCL2 expression in IPF patients[36]. CCL7 is expressed significantly higher levels in biopsies of IPF patients compared to normal samples[39]. Despite the important role

of the chemokines in the pathogenesis of IPF, studies in CCL2 deficient mice and clinical trials of a monoclonal antibody that block CCL2 have failed[40]. These results indicate that chemokines affect the progression of lung fibrosis by activating compensatory actions with each other. CCL12, the analog of CCL2 in humans, was also found to be elevated in the lungs of fibrosis mouse model[40,41]. Compensatory elevations of CCL2 and CCL7 were also observed in CCL12 knockout mice[42]. Lung fibrosis was inhibited in ATII cell-specific CCL12 KO mice and the expression of CCL2 and CCL7 was downregulated in BAL fluid[42]. Therefore, regulation of chemokine signals in ATII cells is critical to the treatment of lung fibrosis. Previous observations and studies have shown that the strategy to block a single chemokine signaling is inefficient, so blocking of EP300 activation in ATII cells, which can prevent compensatory action of C-C chemokines, could lead us to more efficient cures for IPF.

EP300 is an important component of the transcriptional machinery that participates in regulation both at the level of chromatin organization and transcription initiation[16,43]. The expression of EP300 and its functional contribution in physiological responses are controlled by regulation of its cell-type-specific expression, post-translational modification[20]. EP300 also plays an important role in fibrosis and regulates the fibrotic response by controlling homeostasis of the

extracellular matrix, myofibroblast activation and epithelial-mesenchymal transition[12]. The HAT activity of EP300 and its interaction with activated Smads are essential for TGF-β-induced pro-fibrotic signaling[20], demonstrating that EP300 might have a critical role in the progression of tissue fibrosis[17–19]. Although there are increasing studies that ATII cells may play a pivotal role in IPF, the research about the mechanism of EP300 in ATII cell has not been seen prior to this study. Understanding the impact of EP300 on fibrosis in ATII cells will facilitate the design of innovative approaches to control pulmonary fibrosis. Thus, this study sheds light on the functional role of EP300 in alveolar type II cells of chronic lung disease.

In this study, the expression of EP300 is increased in lung tissues of IPF patients and bleomycin-induced fibrosis mouse model compared to normal. Genetic ablation of EP300 in AT2 cells, but not clara cells, prevents BLM and TGF-β-induced lung fibrosis. Importantly, EP300 selectively regulates the transcription of C-C chemokines (CCL2/CCL7/CCL12) in ATII cells, demonstrating that EP300 may act as chemotaxis mediator to promote pulmonary fibrosis in a ATII cell-specific manner. This study offers a conceptual framework for understanding the role of EP300 in ATII cells, with implications for the diagnosis and treatment of IPF.

V. CONCLUSION

Many efforts, including understanding the function of each lung cell and the interactions between cells in the development of pulmonary fibrosis, will improve the overall understanding and treatment results of IPF. In this study, EP300, one of the most studied histone acetyltransferases, was increased in samples of IPF patients and bleomycin-induced mouse models. Immunofluorescence analysis demonstrated that EP300 is increased in ATII cells and club cells among lung epithelial cells in a response to BLM or TGF-β. Using cell type-specific cre mouse of each cell, it was validated that lung fibrosis was selectively inhibited in ATII cell-specific EP300 knockout mice. RNA-sequencing and ChIP-sequencing analyses showed that the transcription of CCL2 and CCL7 are regulated by EP300. TGF-β-induced CCL2 and CCL7 expression were inhibited by knockdown or inhibition of EP300 only in RLE-6TN ATII cell line, but not clara cell, macrophages and fibroblasts. These findings suggest EP300 as a potential therapeutic target for IPF patient's survival and explain the rationale of EP300 inhibition in alveolar type II cell for IPF treatment.

REFERENCES

1. Kinoshita T, Goto T. Molecular Mechanisms of Pulmonary Fibrogenesis and Its Progression to Lung Cancer: A Review. Int J Mol Sci 2019;20:1461.

2. Raghu G., Harold R. C., Jim J. E., Fernando J. M., Juergen B., Kevin K. B., et al. An official ATS/ERS/JRS/ALAT statement: idiopathic pulmonary fibrosis: evidence-based guidelines for diagnosis and management. Am J Respir Crit Care Med 2011;183:788-824.

3. Iwata T., Yoshida S., Fujiwara T., Wada H., Nakajima T., Suzuki H., et al. Effect of Perioperative Pirfenidone Treatment in Lung Cancer Patients With Idiopathic Pulmonary Fibrosis. Ann Thorac Surg 2016;102:1905–1910.

4. Toby M. M., Jeffrey J. S., Michael K., Marlies W., Nicola C., Lucy I., et al. Identifying barriers to idiopathic pulmonary fibrosis treatment: a survey of patient and physician views. Respiration 2018;96:514-524.

5. Rachael C.C., Paul F.M. Mechanisms of alveolar epithelial injury, repair, and fibrosis. Ann Am Thorac Soc 2015;12:S16-20.

6. Ayobami M.O., Xiaoju Z., Hong-Long J. Alveolar type 2 progenitor cells

for lung injury repair. Cell Death Discov. 2019;5:63.

7. Nicole L. J., Jazalle M., Peter M. H., Rubin M. T., Dallas M. H., Rachel L. Z. Unbiased Quantitation of Alveolar Type II to Alveolar Type I Cell Transdifferentiation during Repair after Lung Injury in Mice. Am J Respir Cell Mol Biol 2017;57:519-526.

8. Keira L. W., Monica A. S. Connective tissue growth factor expression and induction by transforming growth factor-beta is abrogated by simvastatin via a Rho signaling mechanism. Am J Physiol Lung Cell Mol Physiol 2004;287:L1323–L1332.

9. Philippe B., Gail M., Peter J. M., Kjetil A., Jennifer R., Jack G., et al. Connective tissue growth factor is crucial to inducing a profibrotic environment in “fibrosis-resistant” BALB/c mouse lungs. Am J Respir Cell Mol Biol 2004;31:510–516.

10. Ivana V. Y., David A. S. Epigenetics of idiopathic pulmonary fibrosis. Transl Res 2015;165:48-60.

11. Ivan O. R., Ivana V. Y. The promise of epigenetic therapies in treatment of idiopathic pulmonary fibrosis. Am J Respir Crit Care Med. 2013;187:336-338.

12. Mingwei L., Yi Z., Huihui Y., Yuan L., Xiaohong W. Effects of dynamic changes in histone acetylation and deacetylase activity on pulmonary fibrosis. Int Immunopharmacol. 2017;52:272-280.

13. Yan Y. S., James S. H., Hui L., Wei Z., Namasivayam A., Victor J. T. Histone deacetylase inhibition promotes fibroblast apoptosis and ameliorates pulmonary fibrosis in mice. Eur Respir J 2014;43:1448-1458.

14. Martina K., Sylwia S., Ingrid H., BreAnne M., Oleksiy K., Shigeki S., et al. Aberrant expression and activity of histone deacetylases in sporadic idiopathic pulmonary fibrosis. Thorax 2015;70:1022-1032.

15. William R. C., Keiria W., Carol A. F., Alan K., Linhua P. Defective histone acetylation is responsible for the diminished expression cyclooxygenase 2 in idiopathic pulmonary fibrosis. Mol Cell Biol 2009;29:4325-4339.

16. Struhl K. Histone acetylation and transcriptional regulatory mechanisms. Genes Dev 1998;12:599-606.

17. Asish K. G., Swati B., Robert L., Giuseppina F., Jianxiu Y., Bayar T., et al. p300 is elevated in systemic sclerosis and its expression is positively regulated by TGF-β: epigenetic feed-forward amplification of fibrosis. J Invest Dermatol 2013;133:1302-1310.

18. Karla R., Indrabahadur S., Stephanie D., Pouya S., Stefan G., Julio C., et al. Inactivation of nuclear histone deacetylases by EP300 disrupts the MiCEE complex in idiopathic pulmonary fibrosis. Nat Commun. 2019;10:1-16.

19. Lee SY, Kim MJ, Jang S, Lee GE, Hwang SY, Kwon Y, et al. Plumbagin suppresses pulmonary fibrosis via inhibition of p300 histone acetyltransferase activity. J Med Food 2020;23:633-640.

20. Chan H.M., La Thangue N.B. p300/CBP proteins: HATs for transcriptional bridges and scaffolds. J Cell Sci 2001;114:2363–2373.

21. Krystian B., Adam J. B., Mateusz J. K., Pawel G., Wojciech J. P. More than a genetic code: Epigenetics of lung fibrosis. Mol Diagn Ther 2020;24:665-681.

22. P H Slee, D De Vos, D Chapman, D Stevenson. The bioavailability of Tamoplex (tamoxifen). Part 3. A steady-state study in breast cancer patients. Pharm Weekbl Sci. 1988;10:22-25.

23. William D. H., Timothy D. L. C., Kenny J., Jay W. T., Mohamad A., Thomas R. K. Conditional expression of transforming growth factor-alpha in adult mouse lung lung causes pulmonary fibrosis. Am J Physiol Lung Cell Mol Physiol 2004;286:L741-749.

24. C. G. Lee, H. R. Kang, Robert J. H., Geoffrey C., Jack A. E. Transgenic modeling of transforming growth factor-β1. Proc Am Throac Soc 2006;3:418-423.

25. Maxim V. K., Matthew R. J., Andrew D. R., Nicolas F. F., Qiaonan D., Zichen W., et al. Enrichr: a comprehensive gene set enrichment analysis web server 2016 update. Nucleic Acids Res 2016;44:W90-97.

26. Jia T., Min Z., Zhijie W., Baoxue W., Lei Z., Yu O., et al. Inhibition of EP300 and DDR1 synergistically alleviates pulmonary fibrosis in vitro and in vivo. Biomed Pharmacother 2018;106:1727-1733.

27. Antje M., Kjetil A., David W., Jack G., Marin K. The bleomycin animal model: a useful tool to investigate treatment options for idiopathic pulmonary fibrosis? Int J Biochem Cell Biol 2008;40:362-382.

28. C. Ramos, M. Montano, J. Garcia-alvarez, B. D. Uhal, M. Selman, A. Pardo. Fibroblasts from idiopathic pulmonary fibrosis and normal lungs differ in growth rate, apoptosis, and tissue inhibitor of metalloproteinases expression. Am J Respir Cell Mol Biol 2001;24:591-598.

29. Norihiko S., Andrea M. T. Fibrosis of two: epithelial cell-fibroblast interactions in pulmonary fibrosis. Biochim Biophys Acta 2013;1832:911-

921.

30. Moises S., Annie P. The leading role of epithelial cells in the pathogenesis of idiopathic pulmonary fibrosis. Cell Signal 2019;66:109482.

31. Venkataramana K. S., Michael K. Lung epithelial biology in the pathogenesis of pulmonary disease. Academic press;2017.

32. Fehrenbach H. Alveolar epithelial type II cell: defender of the alveolus revisited. Respir Res 2001;2:33-46.

33. Wu-Lin Z., Mahboubeh R., Michelle L., Robert J., Sarah L., Jason G., et al. Dysregulation of club cell biology in idiopathic pulmonary fibrosis. PLoS One 2020;17:e0237529.

34. Tetsuya Y., Toyoshi Y., Kunihiro S., Naoki H., Kazuya T., Saiko O, et al. Depletion of club cells attenuates bleomycin-induced lung injury and fibrosis in mice. J Inflamm (Lond) 2017;14:20.

35. Hacer S., Hermann E. W. Chemokines in tissue fibrosis. Biochim Biophys Acta 2013;1832:1041-1048.

36. Christopher P. B., Judy M. O., Sara M., Christie A. N., James M. O., Melissa G. H., et al. Important roles for macrophage colony-stimulating factor, CC

chemokine ligand 2, and mononuclear phagocytes in the pathogenesis of pulmonary fibrosis. Am J Respir Crit Care Med 2007;176:78–89.

37. Suga M., Iyonaga K., Ichiyasu H., Saita N., Yamasaki H., Ando M. Clinical significance of MCP-1 levels in BALF and serum in patients with interstitial lung diseases. Eur Respir J 1999;14:376–382.

38. Paul F. M., Robin H. J., Chris J. S., Malvina A. K., Melanie K., David C. J., et al. Pulmonary epithelium is a prominent source of proteinase-activated receptor-1-inducible CCL2 in pulmonary fibrosis. Am J Respir Crit Care Med. 2009;179:414–425.

39. Esther S. C., Claudia J., Kristin J. C., Steven L. K., Holly E., Fernando J. M., et al. Enhanced monocyte chemoattractant protein-3/CC chemokine ligand-7 in usual interstitial pneumonia. Am J Respir Crit Care Med 2004;170:508-515.

40. Raghu G., Martinez F. J., Brown K. K., Costabel U., Cottin V., Wells A. U., et al. CC-chemokine ligand 2 inhibition in idiopathic pulmonary fibrosis: a phase 2 trial of carlumab. Eur Respir J 2015;46:1740–1750.

41. Jibing Y., Manisha A., Song L., Seagal T., Rachel L. Z., John J. O., et al. Diverse injury pathways induce alveolar epithelial cell CCL2/12, which

promotes lung fibrosis. Am J Respir Cell Mol Biol 2020;62:622-632.

42. Bethany B. M., Lynne M., Anuk D., Carol A. W., Amy B. H., Galen B. T. The role of CCL12 in the recruitment of fiborcytes and lung fibrosis. Am J Respir Cell Mol Biol 2006;35:175-181.

43. Asahara H., Tartare-Deckert S., Nakagawa T., Ikehara T., Hirose F., Hunter T. Dual roles of p300 in chromatin assembly and transcriptional activation in cooperation with nucleosome assembly protein 1 in vitro. Mol Cell Biol 2002;22:2974–2983.

44. Lawryn H. K., Tomofusa F., Michelle A. B., Faycal B., Caili T., Antoine de P., et al. Conditional knockout mice reveal distinct functions for the global transcriptional coactivators CBP and p300 in T-cell development. Mol Cell Biol 2006;26:789-809.

Abstract (in Korean)

폐섬유증에서 히스톤 아세틸화효소 EP300의 Alveolar Type II 세포 특이적 기능 규명

< 지도교수 윤 호 근 >

연세대학교 의과대학 의과학과

이 수 연

가장 흔한 간질성폐질환 중 하나인 특발성폐섬유증은 원인을 모르는 폐 질환이며, 간질 조직에 염증이 반복적으로 일어나게 되면 폐

조직이 딱딱하게 굳어지는 현상인 '폐섬유화'가 일어나는 질병이다. 특발성폐섬유증에 대한 연구는 많이 보고되고 있지만 정확한 분자기전은 알려져 있지 않으며, 섬유화 제거와 생존 연장에 대한 구체적인 치료법 또한 여전히 해결되지 않고 있다. 본 연구에서는 특발성폐섬유증 환자의 폐와 폐섬유화 마우스 모델의 폐에서 EP300의 발현이 증가된 것이 관찰되었다. Cre-loxP 시스템을 이용하여 ATII 세포에만 특이적으로 EP300을 knockout하였을 때 폐섬유증이 억제되는 것을 확인하였다. 그러나 club cell에 특이적으로 EP300을 knockout 하였을 때는 폐섬유증이 억제되지 않아 ATII 세포에서만 EP300이 특이적으로 폐섬유화 진행에 중요한 역할을 하고 있음을 밝혔다. 또 다른 폐섬유증 유도 마우스모델인 *CCSP-TGF*β_1-TG 마우스를 사용하였을 때 역시 EP300이 ATII 세포에 특이적으로 감소하였을 때 폐섬유증 발병이 억제되었다. 이는 ATII 세포에서 EP300이 폐섬유증이 진행되는 데에 중요한 역할을 한다는 것을 시사한다. RNA-sequencing과 ChIP-sequencing 분석을 통해 EP300이 AT2 세포에서 특이적으로 CCL2와 CCL7의 전사 조절 매개함을 알수 있었다. 마우스 폐 조직을 이용한 ChIP assay에서 bleomycin을 처리한

샘플에서는 CCL2와 CCL7의 upstream에 EP300의 결합이 증가하여 CCL2와 CCL7의 전사를 조절하고, EP300이 ATII 세포에서 knock-out됐을 때는 EP300의 결합이 저해되는 것을 관찰하였다. 마지막으로 EP300을 knockdown 시키거나 EP300 inhibitor인 C646을 처리하였을 때 TGF-β_1에 의해 유도되는 CCL2와 CCL7의 발현이 ATII cell에서만 저해됨을 *in vitro*상에서 관찰하였다.

본 연구는 alveolar type II 세포에서 EP300이 폐섬유증 유발에 관여하는 중요하다는 것을 밝혔고, EP300이 특발성폐섬유증 치료에 유망한 타겟이 될 수 있음을 제시한다.

핵심되는 말: EP300, 특발성 폐섬유증, 2형 폐포상피세포, 곤봉체 세포, bleomycin